Classification and Mapping of Saltmarsh Vegetation Combining Multispectral Images with Field Data

Samantha Yeo [a,*], Virginie Lafon [b,†], Didier Alard [a], Cécile Curti [b,†], Aurélie Dehouck [b,†],

Marie-Lise Benot [a,‡]

[a] BIOGECO, Université de Bordeaux, INRA, 33615 Pessac France

[b] GEO-Transfert/ADERA, UMR 5805 EPOC, Université de Bordeaux, Allée Geoffroy Saint

Hilaire, 33405 Talence, France

[*] Present address: Department of Geography, University of California, Los Angeles, CA

90095, USA

[†] Present address: I-SEA, Bordeaux TechnoWest, 25 rue Marcel Issartier, 33700 Mérignac,

France

[‡] Corresponding author: marie-lise.benot@u-bordeaux.fr

Abstract

Salt marshes are areas of high conservation value encompassing diverse ecological gradients responsible for creating unique vegetation structure and composition. In complement to the large body of studies developing vegetation mapping methods through the use of remote sensing data, we tested for the possibility of developing a cost-effective method to map salt marsh vegetation as a basis for monitoring a French Nature Reserve. Using classical multivariate ordination and cluster analyses, accurate and ecologically relevant vegetation groups matching existing typologies were determined from a vegetation database collected for management and conservation rather than mapping purposes. This resulted in six distinct vegetation groups, which were mapped through the combination of the NIR spectral band and radiometric indices (NDVI and NDWI) derived from multispectral 2m-resolution satellite images (Pleiades images). The addition of a LiDAR-derived digital elevation model (DEM) layer was also tested. The final classified map of the reserve based only on optical layers had an overall accuracy of 75.5% (Kappa coefficient of 0.71), with varying success between the different vegetation groups. The addition of the DEM slightly decreased map accuracy to 73.6% (Kappa of 0.68). Decreasing the number of records used for map training had detectable negative effects on map accuracy. This study demonstrated that using already existing field observations combined with only a few spectral bands and radiometric indices from multi-temporal multispectral images with a high spatial resolution can be used as a basis to aid in vegetation classification and mapping of saltmarsh habitats, with the goal of monitoring their dynamics.

10

20

1. **Introduction**

Saltmarshes, complex ecotones forming an interface between aquatic and terrestrial habitats, are considered to be some of the most productive ecosystems in the world (Boorman, 1995). They provide a wide range of valuable ecosystem services (Kelly and Tuxen, 2009) including coastal protection and nature conservation, and offer various socioeconomic activities such as fishing and recreation (Janssen, 2001; Belluco *et al.*, 2006). These habitats, fringing fresh and saltwater ecosystems, are populated by halophytic vegetation adapted to saline and saturated soil conditions (Bertness and Ewenchuk, 2002; Boorman, 2003) exhibiting a strong spatial zonation (Chapman, 1976; Adam, 1990; Marani *et al.*, 2003). Saltmarsh vegetation is a key element in the stability of these areas for their role in the feedback cycle involving hydrodynamic and sediment circulations (Belluco *et al.*, 2006).

Lying at the interface between land and sea, the existence and functioning of saltmarshes depend on the complex relationship of erosion and deposition processes, and are heavily influenced by their biotic components (primarily vegetation), making saltmarshes highly sensitive to environmental changes (Silvestri and Marani, 2004; Lefeuvre *et al.*, 2003). Consequently, these coastal ecosystems face challenges corresponding to increasing global changes, such as anthropogenic activities and rising sea level. The latter has been identified as one of the greatest threats to saltmarsh communities and their ecosystem functioning, impacting sediment retention and accumulation capacities (Adam, 1990; Bromberg *et al.*, 2009; Robins *et al.*, 2016) and shifting vegetation distribution, replacing high saltmarsh species with lower saltmarsh vegetation (Klemas, 2011). In a context of global change, appropriately monitoring saltmarshes and having quantitative and accurate observations of vegetation and their distribution is a critical component for managing these ecosystems and preserving the dynamics of natural communities (Belluco *et al.*, 2006). To reach these conservation objectives, large data-sets of ground data are usually acquired, which first enable

the establishment of a vegetation classification and habitat typology. Such intensive field work is however time-consuming and thus hard to frequently reiterate. Developing operational tools to create accurate maps of saltmarsh vegetation based on the finest possible habitat typology, while limiting the cost and sampling effort, is thus indispensable for documenting and managing these natural areas.

There has been a growing interest in applying remote sensing techniques to mapping saltmarsh vegetation, and studies have shown that it is an effective means of collecting spectral information at a large scale in a noninvasive and cost effective manner (Belluco *et al.*, 2006; Tuxen *et al.*, 2008; Hladik *et al.*, 2013). Additionally, it has been used to map detailed

60　vegetation patterns, distribution, and detect vegetation change (Belluco *et al.*, 2006; Hirano *et al.*, 2003; Silvestri and Marani, 2004; Wang *et al.*, 2007; Klemas, 2011) through synthesizing temporal and spatial dynamics of vegetation patterns (Kelly and Tuxen, 2009). Remote sensing techniques have long been used to monitor saltmarsh vegetation, and the availability of high resolution spectral imagery coupled with improved image processing and classification techniques make mapping increasingly accurate (Kelly and Tuxen, 2009). Fine-scale representation of wetland plant species has proved to be challenging because of the high level of spectral confusion between species (Ozesmi and Bauer, 2002; Schmidt *et al.*, 2004; Tuxen *et al.*, 2011; Hladik *et al.,* 2013). Additionally, wetlands exhibit high spectral and spatial variability which can also complicate mapping vegetation (Wang *et al.,* 2007; Belluco

70　*et al.*, 2006). It is therefore recommended to have a combination of field data (McRoberts *et al.*, 2002; Klemas, 2011; Tuxen *et al.*, 2011) in addition to multi-temporal satellite images in order to acquire information from different vegetation development stages to increase mapping reliability (Belluco *et al.*, 2006). Many studies have previously focused on sites with relatively limited species diversity (see Zhang *et al.*, 1997, 2011), on the quantification of biomass and carbon stocks (see Byrd *et al.*, 2014; 2018) or on the discrimination of broad

vegetation communities or general cover classes (see Kelly, 2001; Andresen *et al.*, 2002; Hirano *et al.*, 2003; Stankiewicz *et al.*, 2003; Smith *et al.*, 1998; Wang *et al.*, 2007; Klemas, 2011; Zhang *et al.,* 2011). In line with the link between saltmarsh vegetation zonation and surface elevation (Pennings and Callaways, 1992; Kulawardhana *et al.*, 2015 and references therein), several studies demonstrate a promising potential of using Digital Elevation Models (DEM) and/or two-frequency laser LiDAR imagery to derive vegetation maps in coastal wetlands (Rosso *et al.*, 2006; Chust *et al.*, 2008; Collin *et al.*, 2010; Owers *et al.*, 2016). In particular, the combination of multispectral images and LiDAR can be an effective way to quantify wetland aboveground biomass and carbon stocks (e.g., Kulawardhana *et al.*, 2014; 2015) or to map wetland vegetation classes (e.g., Rapinel *et al.*, 2015; Ballanti *et al.*, 2017). Additionally, due to the complexity of wetland landscapes, many studies use hyperspectral imagery due to its advantage in spectral resolution (see Hirano, *et al.*, 2003; Rosso *et al.*, 2005; Hladik *et al.*, 2013). However, these sensors can be impractical as their deployment and the analysis of hyperspectral data can be complex and highly expensive (Klemas, 2011, Zhang *et al.,* 2011). Moreover, studies have shown that spatial resolution has a higher impact than spectral resolution (see e.g., Belluco *et al.,* 2006).

Remote sensing has been extensively used for coastal wetland vegetation mapping (Ozsemi and Bauer, 2002). However, it still remains challenging to identify a cost-effective method, which can meet local managers' expectations both in terms of accuracy and ecological relevance. One of the possible limits to using the remote sensing approach is that it requires spatially and temporally accurate field data both for map training and validation. Several strategies of *in situ* data collection have been used to match mapping purposes (e.g., systematic random sampling to cover environmental gradients, Kulawardhana *et al.*, 2014, 2015; stratified sampling from unsupervised classification, Rapinel *et al.*, 2018, etc.). On the

100 contrary, field data formerly acquired for other purposes may not perfectly match remote

sensing requirements, and their relevant coupling is still challenging (Luque *et al.*, 2018).

Thus, the present study addresses the possibility of using an existing vegetation data-set

resulting from an intensive field campaign designed for *in situ* temporal vegetation survey to

create a habitat map of the National Nature Reserve (NNR) of Arès and Lège Cap-Ferret

(Southwestern Atlantic coast of France) through the combination of multi-temporal and

multispectral imagery. Our objective was to test the possibility of developing a simple but

accurate method to map plant communities that could reach local managers' requirements in

terms of vegetation typology. For that purpose, existing vegetation records were used for the

identification and classification of plant communities by the means of classical ordination and

110 cluster analyses, and their unique spectral signatures from satellite images were retrieved

through a Maximum Likelihood Classification (MLC). Possible improvements derived from

the use of additional LiDAR data were searched for. Finally, the effect of a decrease in the

sampling effort of the field data and a reduction of ecological information by aggregating

vegetation groups into broader classes was evaluated.

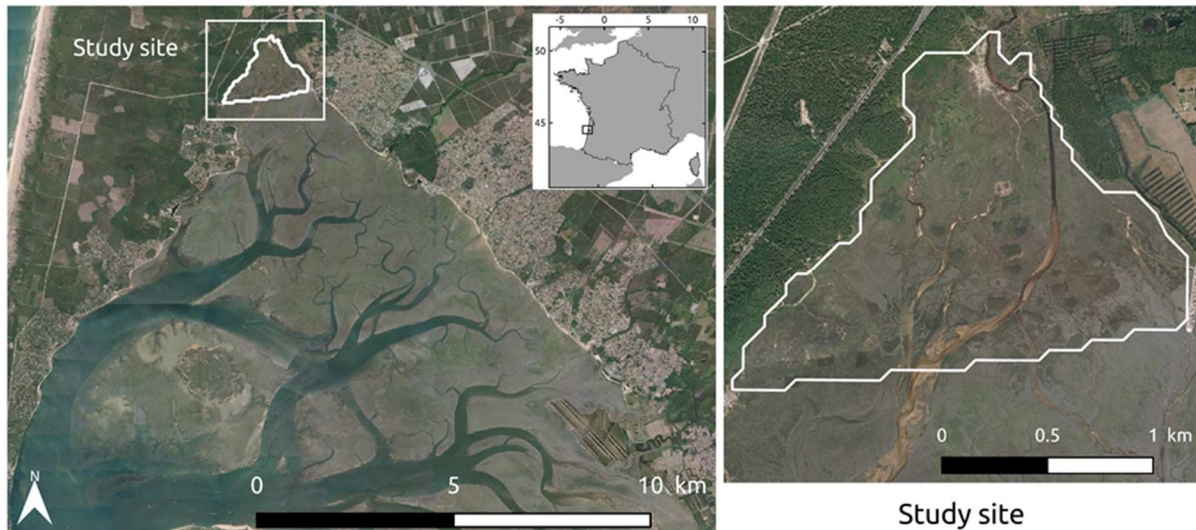## 2. Material and Methods

2.1. Study Area

Fig. 1. Map of the Arcachon Bay (left) showing the location of the study area in Southwestern France. The study site is shown outlined in white (right). Image source: IGN BD ORTHO ® 50cm.

120 This study was conducted in the National Nature Reserve (NNR) FR3600065 of Arès and Lège-Cap Ferret saltmarshes located in the northern tip of the Arcachon bay (France, 44°44'24.06"N; 1° 9'17.78"W), a macrotidal coastal lagoon and the only major indentation in the Southwest coastline of France (Figure 1). The Arcachon bay represents one of the most important oyster farming areas and tourist destinations in France. The Reserve occupies an

125 area of 320 hectares and is home to the largest saltmarsh area in Southwestern France. Hydrologically, the Reserve is under the dual influence of saltwater from the Atlantic Ocean and freshwater from upstream freshwater lakes connected to the bay by a canal ("*Canal des Etangs*"), creating a gradient of salinity from the sea moving progressively inland. This factor contributes to the organization of plant communities ranging from the slikke (mudflats) to the

130 schorre (saltmarsh) and finally transitioning to the foot of the sand dune where woody communities can be found. In addition to vegetated areas, the saltmarsh of the Reserve includes areas of bare sand, mudflats and artificially created hunting ponds.

The Reserve is part of the European Natura 2000 site FR7200679 "*Bassin d'Arcachon et Cap Ferret*" (Reveillas *et al.*, 2012). This site was chosen because it is one of the few

saltmarshes in France with a diversity of habitats containing the complete gradient from slikke to schorre.

2.2. Field Data and Treatment

Fieldwork was conducted between the months of June and September in 2011 on the saltmarsh of the Reserve (Reveillas *et al.*, 2012). The sampling strategy was designed to build a temporal *in situ* survey of vegetation dynamics based on a spatially explicit method covering the extent of the Reserve under tidal influence. Survey sites were regularly distributed based on a 50m grid superimposed on the entire site extent, with each floristic record performed at the intersection of the axes of the grid. This resulted in a total of 832 survey points across 193.43 hectares covering the elevation gradient from the slikke to the schorre. The survey points were comprised of 16m² records with their x and y coordinates defined *a priori* and found on site during the survey using a GPS with about 5m average accuracy (Garmin® 62S). Each record contained five 1m² quadrats: one in each corner and one in the center. In each quadrat, coefficients of abundance and cover for each detected plant species were noted. By averaging the values in each of the five 1m² quadrats, species' abundance was then evaluated for the entire record. The cover of bare soil was also taken into account in each of the 1m² quadrats for each record. The notation used for species abundance and bare soil corresponds to the dominance scale (Hill *et al.*, 2005) and varies from one (less than 4% of vegetation cover or bare soil) to 10 (91-100% vegetation cover or bare soil).

The original dataset was treated following several steps in order to keep only floristically homogenous records suitable for the mapping purpose. First, out of the 832 vegetation records initially planned, 156 were not visited in the field as they were positioned on bare soil, resulting in a total of 676 vegetation records in the database containing 68 plant species (see Table S1 for the complete species list). Correspondence analyses (CAs) were

160   used to identify the main gradients that structure species' assemblages and were followed by hierarchical clustering (HAC, Ward's method using Euclidean distance among records calculated from coordinates along the first three CA axes) to discriminate vegetation groups along these gradients. A first analysis allowed 12 groups of records to be discriminated on the basis of their floristic composition. Six of these groups were removed (representing 30

165   records) as they either had too few records or were considered to be outliers on the gradient due to the presence of rare species. Plant species that were not representative of Atlantic and Continental Saltmarshes (Natura 2000 codes 1310-1330; six species, see Table S1) were also removed for data treatment. Then, floristically heterogeneous records were removed as they were expected to have a fuzzy spectral signature that would negatively impact pixel

170   classification. In that purpose, a Bray-Curtis (BC) dissimilarity index was calculated for each record as the average Bray-Curtis distance among each pair of quadrats contained in a record (five quadrats per record leading to ten Bray-Curtis distances). This index was used to determine the floristic dissimilarity amongst the quadrats in a record based upon species composition, in order to determine floristically homogeneous or heterogeneous records. The

175   index ranges between 0 and 1; 0 being exactly similar intra-record species composition and 1 meaning that the quadrats within a record share no species. A threshold of 0.1 was established as a limit of homogeneity, and records with a BC score superior to 0.1 were not retained (194 records). Finally, low frequency species (species present in only one or two records, 27 species) were removed. All of these manipulations led to a final database of 452 records

180   containing a total of 35 species (Table 1; see also Table S1 for the list of the remaining species).

Table 1. Phytosociological categories (alliance or association) and Natura 2000 habitat codes (N2000 Code) for the identified vegetation groups. Group codes and generic names are provided for each determined thematic class in addition to the total number of ground records and the maximal number of records remaining for map training.

Group code	Generic name	Alliance	Association	N2000 Code	Total number of records	Maximal number of training records
Six groups						
A	Top level Atlantic saltmarsh and grass communities	*Agropyrion pungentis*	*Atriplici hastatae-Agropyretum pungentis*	1330-5	42	22
B	High schorre communities	*Agropyrion pungentis*	*Agropyro pungentis-Inletum crithmoidis*	1330-5	95	75
C	Mid schorre communities	*Halimionion portulacoidis*	*Halimionetum portulacoidis*	1330-2	104	84
D	High Atlantic slikke communities	*Salicornion dolichostachyae*	*Astero tripolii-Suaedetum maritimae / Salicornietum obscurae*	1310-1	51	31
E	High slikke *Spartina maritima* swards	*Spartinion anglicae*	*Spartinetum maritimae*	1320-1	72	52
F	High slikke *Spartina anglica* pioneer communities	*Spartinion anglicae*	*Spartinetum anglicae*	-	88	68
Five groups						
CD	Low-mid schorre communities	*Halimionion portulacoidis*	-	1330	155	135
Four groups						
AB	Top level and high schorre communities	*Agropyrion pungentis*	-	1330-5	137	117
Total					**452**	**-**

A final CA was applied to the filtered database, followed by a hierarchical clustering of the records based on their scores along the CA1 and CA2 axes (Ward's method). Vegetation groups were determined by cutting the dendrogram initially to form six groups. Then to progressively merge the vegetation groups, the dendrogram was cut at higher levels forming five and four groups (Figure S2). The Indicator Value (IndVal), a quantitative index of the fidelity and specificity of a species to a group, was calculated for each species in the determined vegetation types (Dufrêne and Legendre, 1997). Only indicator species that were statistically significant (p-value < 0.05) with an IndVal greater than 0.2 were retained. On the basis of indicator species, each vegetation group was then identified and classified within a phytosociological typology (alliances and associations) following vegetation syntax described by the Provisional Reference Typology for Natural and Semi Natural Saltmarsh Habitats in Aquitaine by the French National Botanic Conservatory of South-Aquitaine ("*Conservatoire Botanique National Sud-Atlantique*", CBNSA). When relevant, the N2000 habitat codes were also documented (Table 1).

All statistical analyses were carried out using R 2.15.2 (R Development Core Team 2016; http://www.r-project.org/). Packages used included vegan (Oksanen *et al*., 2016), Ade4 (Dray and Dufour, 2007), labdsv (Roberts, 2016), and agricolae (de Mendiburu, 2016).

2.3. Multispectral Image Acquisition, Processing and Spectral Band Selection

Very high resolution multispectral images were acquired by the Pleiades Satellite 1B via a research dedicated program developed by the French National Center for Space Studies (CNES) for the site of the reserve on four different dates: April 14th and 25th, August 21st, and December 4th in 2013. Each image provides 2m ground resolution and 4-band multispectral (blue, green, red, and near-infrared/NIR) products, making a total of four multispectral images with 16 combined bands. The images for August and both dates in April were georeferenced

by IGN (French National Institute of Geographic and forest information) to the French Geodetic Network (RGF93) system and the Lambert-93 projection. The image for December was georeferenced by hand using well distributed ground control points (GCPs). No atmospheric corrections were made on the images, and all four images were cloud free. Two indicators, the *Normalized Difference Vegetation Index* (NDVI, Rouse *et al.*, 1974) and *Normalized Difference Water Index* (NDWI, McFeeters, 1996), were calculated for each date of the satellite images to facilitate the detection of vegetation and water in the study area, creating an additional eight bands. A Kruskall Wallis rank sum test, with the vegetation groups as the main factor, was used to determine the bands that most easily discriminated the groups according to their numeric pixel values. The subset bands for which the Kruskall Wallis rank sum test detected a significant difference (p-value < 0.05) between vegetation groups were selected. The values of the four 2x2m pixels representative of the vegetation records were extracted for each band by creating 16m² square buffers around each GPS point. Finally, only NIR, NDVI and NDWI bands were retained for the four dates as they were statistically found to discriminate the best vegetation groups (see Figure S1 for a visual representation of the retained bands) and combined into a single false color composite image.

2.4. LiDAR data Acquisition and Processing

In December 2011, the Intercommunal Union for the management of the Gironde pond watershed ("Syndicat intercommunal d'aménagement des eaux du bassin versant des étangs du littoral girondin", SIAEBVELG) acquired the LiDAR data for the study site. Data was collected with a LiteMapper 6800 mounted in a Cessna 206 (F-GDAP) flown at an altitude of 500m above ground level. The survey was conducted with a laser PRF of 200 kHz with a total field of view of 60 degrees and a target point density of 3.8 laser points per m² (Parallele 45

Géomètres-Experts Associés, Lacanau, France). From this data, a digital elevation model (DEM) was derived (2 meter pixel resolution), creating an additional band (25 bands in total).

2.5. Classification Method

A Maximum Likelihood Classification (MLC) was then applied on the false color composite image with and without the DEM layer in order to create spectral signatures for each vegetation group defined by the typology and to assign each pixel to a given vegetation group. For the classification, two subset groups of the records were created (Wang *et al.*, 2007): one to be used as a training group and the other as a validation group. The training and validation samples for the classification were defined by the range of pixel values contained in each record, which were then assigned to the vegetation group to which the corresponding record belonged.

For the validation group, 20 records were randomly selected from each defined vegetation group to test the accuracy of the map. This number remained constant for each group in each classification. The records selected were evenly spaced according to the ecological gradient created by the CA (CA1 axis) and dispersed in the study zone in order to represent the full range of intra- and inter-group variability. This number was obtained for the sample size from Hay (1979) who concluded that a minimal sample size of 50-100 pixels per established group is recommended for accurate validation (Janssen, 2000). Each 16m² vegetation record contains four pixels, making a total of 80 pixels for validation per group.

For the training samples, the remaining records independent of the validation groups were selected at 10% intervals ranging from 100% (all the remaining available records of each vegetation group) to 10% in order to assess the effect the sample effort on the overall accuracy. These records were randomly reselected for each group for each percentile of degradation in order to define a range of variance of pixels representative of each vegetation

group to be used in the image classification. The training records were also evenly spaced along the ecological gradient and dispersed throughout the study site. As no record was acquired *in situ* for sampling sites containing no vegetation, training samples of water (including channels and hunting ponds), bare mudflat, and sand were manually delineated by photo-interpretation and were included in the classification in order to increase spectral differentiation of the Reserve. The data-set did not include any validation samples for these habitats.

A total of 60 classifications were examined for six, five, and four vegetation groups, both with and without the DEM data, with the training sample effort diminishing in 10% intervals. A post-classification Majority Filter using the eight nearest neighbors was applied on the classified habitat maps in order to smooth out erroneously classified pixels and reduce the "speckle" effect. The validation samples were then used to test the accuracy of the smoothed maps in predicting the vegetation groups across the study site.

ArcMap version 10.2.1 software program (http://www.esri.com) was used for all image analyses, indicator calculations, and classification processes.

2.6. Accuracy Assessment

Quantitative standard accuracy measurements to assess the classified maps is based on the Confusion Matrix, in which the Kappa coefficient (K), overall accuracy, producer's accuracy, and user's accuracy for each vegetation group were calculated using the error matrix method on the final smoothed images (Congalton, 1991). The Kappa coefficient (K), a discrete multivariate technique used in accuracy assessment, is a measure of accuracy in which 0 means an accuracy of less than what would be expected by chance and 1 is perfect accuracy (Viera and Garrett, 2005). Overall accuracy (A) is computed by dividing the sum of the total correct classified pixels by the total number of pixels in the vegetation groups. For each

classified map, the percent of the standard error for the overall accuracy (and the Kappa coefficient) was calculated, using the formula:

$$SE(\%) = \sqrt{\frac{p(\%)q(\%)}{n}}$$

in which p is the overall accuracy (or the Kappa coefficient), q is 1-p, and n is the total number of pixels in the classification. The percent of the standard error was calculated for each classification map, and all errors were rounded to whole numbers or to the nearest tenth. Producer's accuracy (or omission error) indicates the probability of a pixel being correctly classified, and is calculated by the total number of correct pixels found in a vegetation group divided by the total number of pixels of that group as derived from the ground data. Finally, the user's accuracy (or commission error), a measure indicative of the probability that a pixel classified on the map actually represents that category according to the field data, is calculated by dividing the total number of correct pixels in a vegetation group by the total number of pixels that were classified in that group (Congalton, 1991).

3. Results
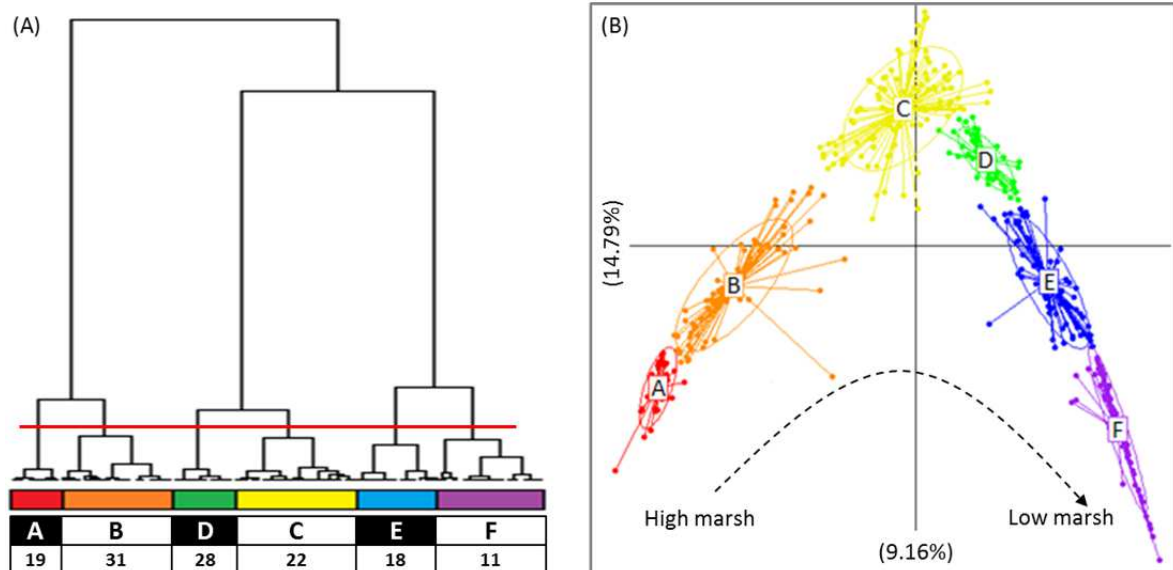
3.1. Vegetation Records and Groups

Fig. 2. (A) Hierarchical Classification performed on the [452 records x 35 species] data table. The red line indicates the level where the dendrogram was cut to define six clusters (named A-F) used for the associations. (B) Correspondence analysis on the F1-F2 factorial plan of the records showing the vegetation groups (defined in the Hierarchical Classification). Habitat turnover from high to low marsh is visualized by the arrow.

Using the nomenclature provided by the CBNSA, the six distinct vegetation groups defined

300   from using the 452 vegetation records and 35 species of the final data table and their

corresponding indicator species (Figure 2, see Table S1 for corresponding names to species

codes) were classified into five phytosociological alliances and six associations (Table 1). The

vegetation groups present a clear spatial gradient permitting to visualize the typical zonation

patterns of saltmarsh plant communities from the high schorre featuring top level Atlantic and

high schorre communities (designated as groups A and B) to the slikke, containing *Spartina

maritima* swards and *Spartina anglica* pioneer communities (groups E and F) (Table 1, Figure

3). When the dendrogram was cut at higher classification levels, groups C (mid schorre

communities) and D (high Atlantic slikke communities) were first merged, leading to a

rougher group. Then, both A and B groups were merged (Table 1, Figure S2).

310   Most of the 196 vegetation records considered floristically heterogeneous according to the

Bray-Curtis dissimilarity index were located (i) within vegetation groups B, C, and D (high

schorre, intermediate schorre, and high slikke respectively), (ii) at the interface between these

groups or (iii) at the interface between these groups and groups A (high schorre) or E (high
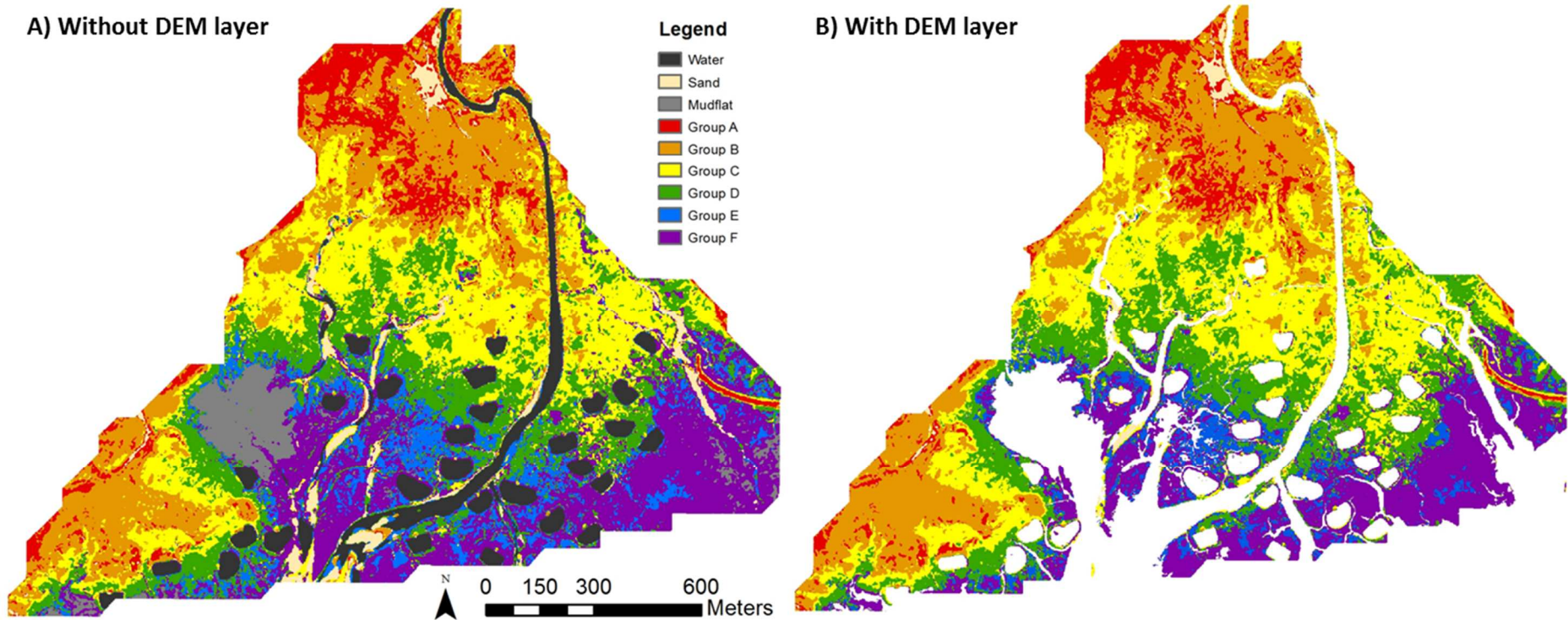
slikke) (Figures S3 and S4).

Fig. 3. Maximum likelihood classification (MLC) maps (after application of the post majority filter), obtained using 100% of the remaining available records for the training groups (A) only with optical layers (overall accuracy: 75.5%) and (B) with optical and digital elevation model (DEM) layers (overall accuracy: 73.6%). The six vegetation groups in addition to water bodies (channels and hunting ponds), sand, and mudflats are featured. No LiDAR data were available for water bodies and mudflats, which do not appear on the resulting map (B).

3.2. Quantitative Map Accuracy

Table 2. Interactive Supervised Classification (ISC) error matrix of the final map using 100% of the remaining available records for the training groups (A) only with optical layers and (B) with optical and digital elevation model (DEM) layers. Columns represent the reference data (what the pixel actually was based on validation data) and rows represent the image data (what the pixel was classified as). Shaded cells show the correctly classified pixel observations for each association. Results are in total number of pixels, while the producer and user's accuracy are in percentage.

(A) Without DEM layer

Ground Data	A	B	C	D	E	F	User's Accuracy
Map Data							
A	**51**	10					84%
B	29	**70**	10	4			62%
C			**53**	4		1	91%
D			17	**51**	5	2	68%
E				7	**69**	8	82%
F				14	6	**66**	77%
Producer's Accuracy	64%	88%	66%	64%	86%	86%	*Overall Accuracy: 75.5%* *K = 0.71*

(B) With DEM layer

Ground Data	A	B	C	D	E	F	User's Accuracy
Map Data							
A	**48**	9					84%
B	32	**70**	7	4			62%
C			**54**	8		2	84%
D			19	**47**	5	2	64%
E				7	**64**	7	82%
F				14	6	**56**	74%
Producer's Accuracy	60%	89%	68%	59%	85%	84%	*Overall Accuracy: 73.6%* *K = 0.68*

When 100% of the classification records were used, the map representing the six vegetation groups reached an overall accuracy of 75.5% (K= 0.71) for the optical and DEM classification (Table 2A). User's accuracy was the highest for vegetation group C (91%), intermediate for

groups A, E and F (77% - 84%) and the lowest for groups B and D (62% and 68%). Variations in Producer's accuracy were different with the highest values obtained for group B (88%), E and F (86%) and the lowest values for groups A, C and D (64 – 66%; Table 2A). These values were overall lower when DEM was included in the classification (Table 2B).

The best classification results were obtained for the five vegetation groups, when 100% of classification records were used, having overall accuracies of 83.6% (K= 0.8) and 82.4% (K= 0.78) for the optical and DEM classifications, respectively. The results show that including the DEM layer in the classification systematically results in lower A and K values for all groups in all categories, with the exceptions of when 10% and 30% of records were selected for the five and six vegetation groups in which the A and/or K values are slightly higher after the addition of the DEM layer (Table 3, Figure 4, Appendix S2).

Table 3. Overall accuracy assessment (%) of the classification results for six, five, and four vegetation groups, with and without digital elevation model (DEM) layers.

Input Variables	Remaining Records Used in Training Sample (%)									
	100	90	80	70	60	50	40	30	20	10
Six Groups										
Optical	75.5	67.0	65.9	68.4	68.2	62.1	60.8	53.3	49.9	9.6
Optical + DEM	73.6	62.0	58.4	61.1	64.1	58.0	52.8	52.3	47.9	18.6
Five Groups										
Optical	83.6	73.5	72.6	76.0	78.0	70.6	68.2	58.7	57.5	17.1
Optical + DEM	82.4	70.0	67.2	67.1	73.2	66.1	63.9	59.0	50.4	21.2
Four Groups										
Optical	80.1	81.0	81.0	80.4	80.7	81.1	77.5	75.7	75.8	57.5
Optical + DEM	76.7	72.2	76.7	70.6	76.3	77.7	69.2	70.0	73.4	54.2

For each vegetation group, the validation sample comprised 20 vegetation records.

330

Generally, the results show higher A and K values with an increasing percentage of classification records used, coupled with decreasing the number of vegetation groups, despite a few exceptions (Table 3, Figure 4).
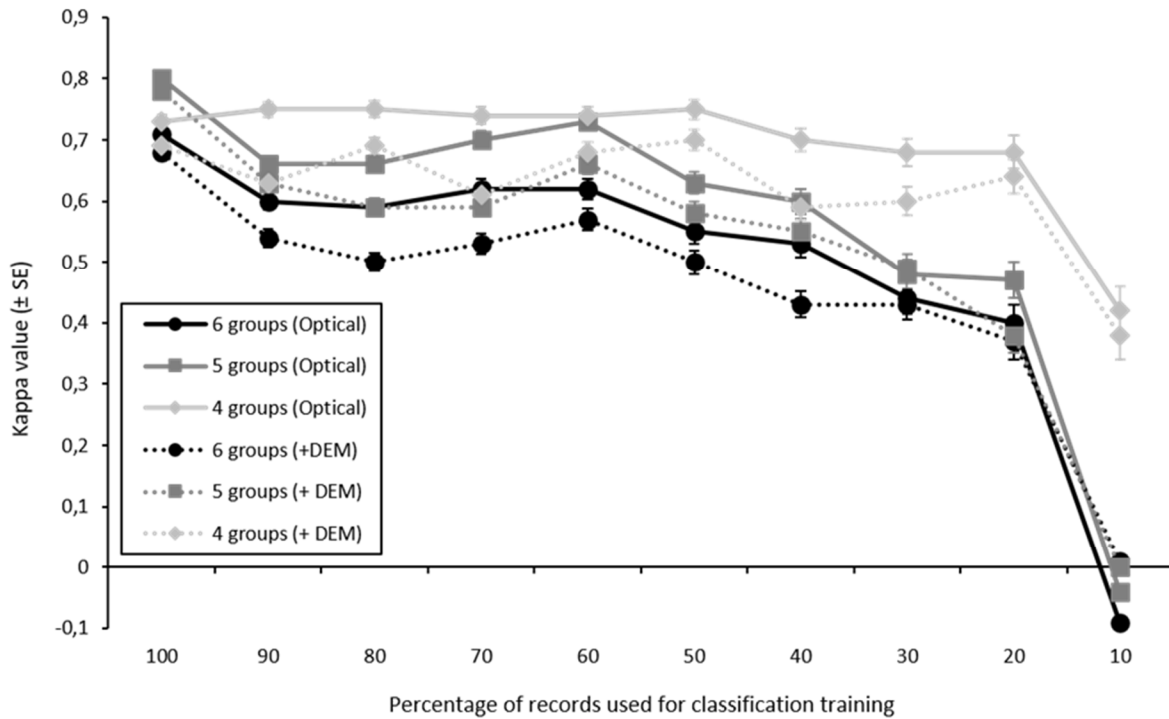
Fig. 4. Comparison of obtained *K* values for the six, five, and four vegetation groups with (dashed lines) and without (solid lines) digital elevation model layer. Bars represent the standard error of the *K* values for the classifications.

For the six and five vegetation group categories, the trends in the A and K values for both optical and DEM classifications follow the same fluctuational tendencies (Table 3, Figure 4). The K values for these two groups decrease when reducing the number of records used for map training from 100 to 90%, remained rather constant from 90 to 60%, then steadily decrease with reducing the sample effort to 20%. The MLC accuracy performed with four vegetation groups however, does not follow this general tendency. The K values are stable when the sample effort ranges between 100-50%, and slightly decrease when reducing the sample effort to 20%. Regardless of the number of vegetation groups, decreasing the percentage of classification records down to 10% corresponds in a very small number of records for some classes, ranging between 2 records (8 pixels) for class A and 14 records (56 pixels) for class CD (Table 1). This has severe consequences on the map training, as shown by

350 collapses in overall accuracy and null to negative Kappa values (Table 3, Figure 4), and the failure to map some of the vegetation groups (Appendix S2). Reducing typology accuracy to only four vegetation groups prevented this dramatic effect (Table 3, Figure 4).
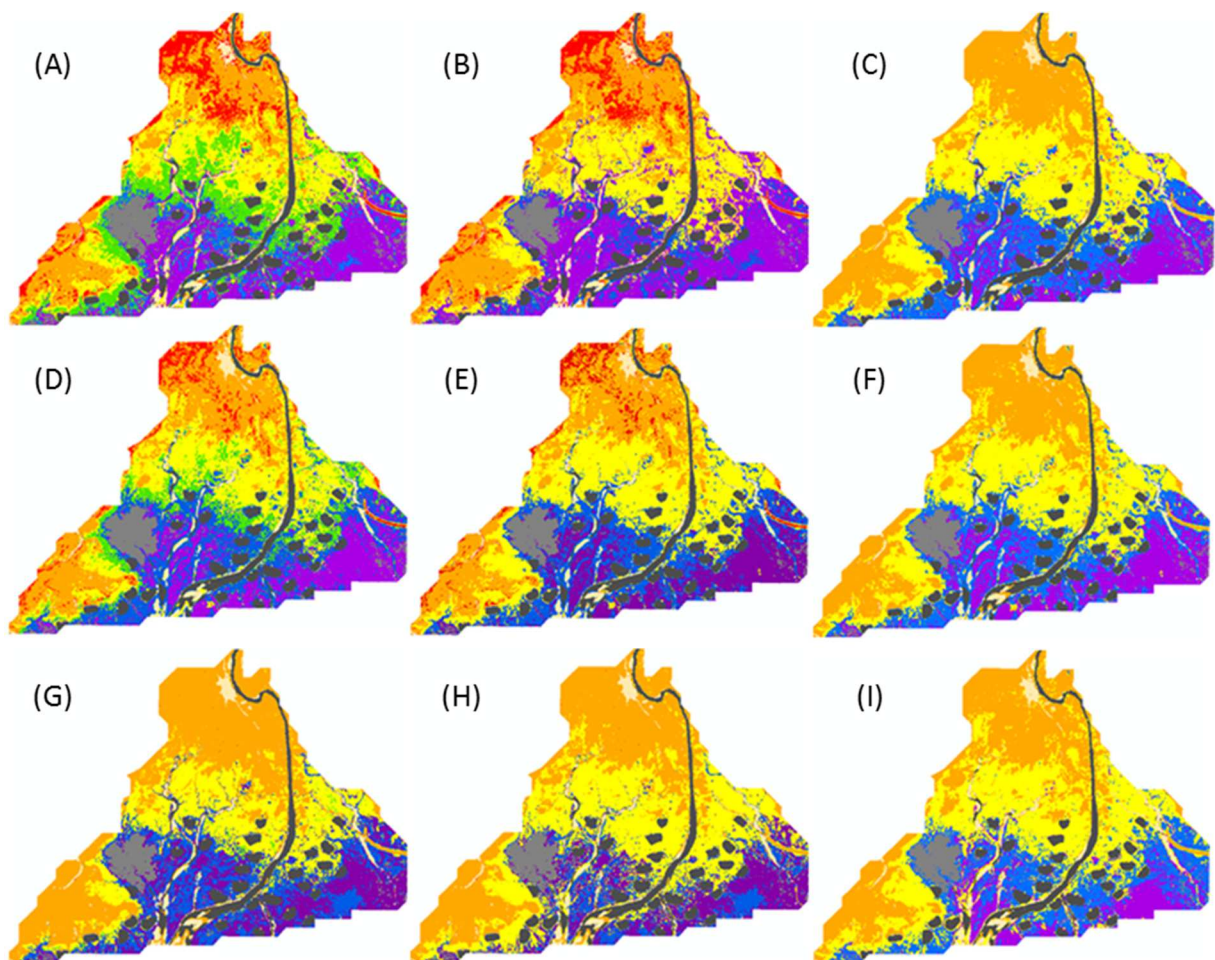
3.3. Qualitative Map Accuracy

355

Fig. 5. Maximum likelihood classification maps demonstrating results for 100% (top), 50% (middle), and 20% (bottom) of the remaining available records for the training groups for the six (A, D, G), five (B, E, H), and four (C, F, I) thematic classes. Only classifications including optical layers are shown.

For purposes of brevity, nine out of the sixty classifications were chosen to demonstrate general trends for the classification results (100%, 50%, and 20% intervals for the three group categories for the optical classification; Figure 5). From visual interpretation of the vegetation

360   groups, all classifications demonstrated the distribution of vegetation groups in the final

classified products to be generally consistent with typical zonation patterns of saltmarshes and

more specifically represented by the field records, showing the gradation from high schorre to

slikke (Figure 5), with exception to the 10% category (not shown) for five and six vegetation

groups. In reducing the percentage of records used in the training sample, certain spectral

365   groups become more dominant while others become less prominent, or completely disappear

(e.g., group A with 20% of training samples and six vegetation groups, Figure 5G, Appendix

S2). However, regardless of the quantity of records, the maps produced exhibit an overall

agreement with the general spatial patterns of the observed records.

370   **4. Discussion**

Complementary to previous studies aiming at mapping saltmarsh plant communities, we

developed an approach combining robust but already existing field data collected for other

purposes than vegetation mapping with multi-date multispectral imagery. This approach

proved efficient in capturing the full gradient of saltmarsh vegetation, from the slikke to the

375   schorre, deriving a complete vegetation typology and mapping of these vegetation groups.

The classification results show that the mapping method devised from hierarchically

classifying vegetation into groups derived from a complete habitat typology is generally in

quantitative and qualitative agreement with observed field data. The overall classification

accuracy of the most complete map (i.e., using 100% of available records for map training

380   and 6 vegetation groups) was rather high (75.5%) with a moderate Kappa coefficient of 0.71

(see Viera and Garrett, 2005 for Kappa interpretation scale). Both producer's and user's

accuracies varied according to the vegetation group considered. The producer's accuracy was

the highest for groups B (high schorre communities), E, and F (high slikke *Spartina maritima*

swards and *S. anglica* pioneer communities), ranging from 86-88%, with group B being the

385   best classified. From a user's perspective, the most accurate groups were groups A (top level Atlantic saltmarsh and grass swards), C (mid schorre communities), and E (high slikke *S. maritima* swards), with a user's accuracy reaching 91% for group C. These results imply that the detailed spectral information provided by the multispectral image data may be particularly effective for differentiating vegetation groups in the upper and lower marsh.

390   However, in the intermediate marsh (mostly low schorre and high slikke), the classification was less accurate. Vegetation group D (high Atlantic slikke occupied by *Salicornia* species) had the lowest scores (user's and producer's accuracies of 64 and 68% respectively), showing that there is significant spectral confusion in discriminating this cluster from other clusters. Using hierarchical methods to classify vegetation groups from a robust data-set spanning the

395   entire study site allowed us to build a thorough habitat typology, therefore reducing uncertainties of the data. Vegetation typology and the way by which it is built may affect vegetation group mapping. In wet grasslands, Rapinel *et al.* (2018) demonstrated that a compromise of vegetation typology based on both floristic and spectral information provided a better accuracy than classic phytosociological typology. In the present study, only floristic

400   composition was used to classify vegetation composition, using classical ordination and cluster analyses. Although this may have decreased mapping accuracy, as suggested by Rapinel *et al.* (2018), our approach enables the ability to build a typology that can match local managers' knowledge and conservation needs, independently of the acquisition of remote sensing data. Other studies on supervised image classification for precisely defined vegetation

405   classes such as phytosociological associations are rare, however one study combining hyperspectral imagery with field samples collected using the Braun-Blanquet method to classify and map vegetation groups had an overall accuracy of 40% with a Kappa coefficient of 0.35 (Schmidt *et al.*, 2004). This same study also showed that by combining ancillary data to the classification, such as height, slope, aspect, and terrain position, the classification

accuracy improved to 66% with a Kappa coefficient of 0.64. Using supervised classification for general cover classes based on four saltmarsh dominant species in the Lagoon of Venis, Belluco *et al*. (2006) reported accuracies ranging from 74.6-96.1% with Kappa coefficients ranging from 0.67-0.86. These high accuracies are typical with broad cover classes, as supervised classifications have been shown to have higher performance when fewer classes are distinguished (Janssen, 2001). In our study, the use of multi-temporal, although opportunistically acquired, Pleiades images certainly contributed to the improved map accuracy as it enables the integration of phenological differences between vegetation groups, thereby increasing their spectral discrimination.

Increasing spatial and spectral resolutions have been proposed to increase mapping efficiency. Using images with higher spatial resolution presents the advantage of having a larger number of reference pixels to be used in the classifier training, and therefore increasing the spectral separability of classes (Janssen, 2001; Hladik, 2012). This is a particularly important advantage in the case of highly heterogeneous vegetation communities (Belluco *et al*., 2006) where under-represented classes can be lost in the mixed pixels when performing a supervised classification (Hladik, 2012). In our study, all of the four pixels constituting a vegetation record were assigned to the vegetation group defined at the scale of this record. Thus, floristically heterogeneous records, which represented almost 30% of the 676 records containing vegetation, were removed from the analysis as they were thought to have fuzzy spectral signatures that could have impacted classification accuracies. Floristically heterogeneous records indicating small scale (i.e., less than 16m²) heterogeneity were found all along the slikke to schorre gradient, both within vegetation groups and at the boundaries between vegetation groups (Figures S3 and S4). As it was removed from the analysis, such heterogeneity cannot explain differences in map accuracy. For instance, group C (mid schorre) appears to be the one in which the largest number of heterogeneous records are found, but it is

435 also the group with the highest user's accuracy. Similarly, group B (high schorre), for which we obtained the highest producer's accuracy, also contained several heterogeneous records. Thus, for these groups, small-scale floristic heterogeneity (i.e., at the record scale) did not affect classification quality. On the contrary, group D (high Atlantic slikke) was the least well represented group. Rather than small-scale floristic heterogeneity, a sort of "ecological

440 heterogeneity" within records located at the interface between two vegetation groups could be responsible for misclassification. Several factors other than floristic composition, which we used for vegetation typology (e.g., proposition of bare soil, water content, biomass), can lead a single vegetation group to be characterized by several spectral signatures (Rapinel *et al.*, 2018). Indeed group D is a spatially complex mosaic narrow habitat at the transition between

445 groups C (mid schorre) and E (high slikke *S. maritima* swards), represented by the smallest number of vegetation records. Defining a clear signature from this group proved challenging. Other studies have also shown that, in heterogeneous areas of saltmarshes, supervised classifications are generally unable to classify under-represented classes and mixed pixels (Belluco *et al.*, 2006). Increasing sampling effort within this vegetation group would thus be

450 required to try and increase the accuracy of its mapping. Additionally, positional discrepancies in the referenced data due to accuracy errors of the GPS should also be considered. These differences could have resulted in a slight shift in the position of the records on the map, leading to a misrepresentation of pixels.

Increasing spectral resolution of the satellite images by using hyperspectral imagery

455 instead of multispectral imagery could also improve the identification of saltmarsh associations. Hyperspectral images are able to collect a high number of continuous spectral bands (sometimes greater than 200) and allow for better species differentiation when compared to multispectral imagery (Belluco *et al*., 2006; Hladik, 2012). However, studies have shown that there is a redundancy in the information of hyperspectral bands, creating a

460   tradeoff between the number of spectral bands chosen and the accuracy of the classifier, therefore the number of spectral bands chosen must be limited. Additionally, although higher spectral resolution yields more accurate results, studies have shown that having higher spatial resolution is more important than higher spectral resolution (Belluco *et al.*, 2006).

        In the present study, the Pleiades images used were opportunistically recorded and

465   dates were not chosen with a specific aim. Another study in the Arcachon bay defined the potential of using long term time-series of satellite imagery to derive exhaustive maps of intertidal and saltmarsh habitats (Lafon *et al.* 2014), demonstrating that good quality maps were obtained by fusing the results of the Mahalanobis Distance classifier applied to SPOT5 imagery acquired from winter to summer 2011 to Iterated Conditional Modes (ICM)

470   classification results derived from Synthetic Aperture Radar (SAR) seasonal acquisition. They also showed that imagery obtained in the springtime is particularly advantageous in distinguishing species and assemblages, therefore, Pleiades images from April are of great interest. It is also important to consider the difference in the dates of data acquisition, as the remotely sensed imagery was taken two years after the field surveys were conducted. As

475   saltmarsh vegetation is dynamic, vegetation patterns are subject to change rather quickly (Janssen, 2001). Using synchronized field samples and satellite images could have potentially different classification results.

    Identifying boundaries in which one vegetation group stops and another begins is often difficult, especially in saltmarsh communities which exhibit mixed vegetation types blending

480   into one another (Kelly and Tuxen 2009). In our study, this heterogeneity was detected in almost 30% of the vegetation records, suggesting that about one third of the vegetation surface is likely to be hardly assigned to one vegetation group or another. Previous research has shown that it is difficult to classify saltmarsh plant communities by purely using their spectral signatures (Zhang, *et al.*, 2011) therefore many studies use a combination of satellite

485 images with topographic and edaphic data to increase classification accuracies (see Schmidt *et al.*, 2004; Tuxen and Kelly 2009; Hladik, 2012; Hladik *et al.*, 2013) and verify the accuracies afterwards with a select number of field samples. Saltmarsh vegetation exhibits a strong spatial structuration (Chapman, 1976; Adam, 1990; Marani *et al.*, 2003) and it is well established that inundation frequency and elevation are the primary determining factors for

490 these patterns (Adam, 1990; Boorman, 2003; Silvestri and Marani, 2004; Wang *et al.*, 2007; Bilodeau, 2010). Studies show that incorporating elevation data improves the accuracy of saltmarsh aboveground biomass or carbon stock quantification (Kulawardhana *et al.*, 2014; 2015), in addition to saltmarsh (Klemas, 2011; van Beijma *et al.*, 2014; Owers *et al.*, 2016), as well as other wetland habitat mapping (Rapinel *et al.*, 2015; Ballanti *et al.*, 2017; Rapinel *et*

495 *al.*, 2018). On the contrary, our results show that adding LiDAR-derived DEM layer to optical information generally decreased overall map accuracy. This suggests that LiDAR data used in the present study were not accurate enough to detect sharp variations in altitude. In our study, LiDAR data were used to derive a DEM, while classification improvements provided by LiDAR data do not strictly rely on the accurate description of elevation, but also on the use of

500 LiDAR data to characterize three-dimensional vegetation structure (Kulawardhana *et al.*, 2017), which may help in defining vegetation groups. Moreover, several factors can affect LiDAR accuracy such as sensor resolution or vegetation density, which may limit laser penetration (Hladik, 2012). DEM derived from raw LiDAR data may not be accurate enough for flat vegetated habitats such as those targeted in the present study (Chust *et al.*, 2008;

505 Fernandez-Nunez *et al.*, 2017). Indeed, poorer vertical accuracy is found for taller vegetation (Hladik and Alber, 2012). The application of species or habitat-specific correction factors (e.g., vegetation height or aboveground biomass density) greatly improves the accuracy of the LIDAR-derived DEM (Hladik and Alber, 2012; Fernandez-Nunez *et al.*, 2017). Corrections are thus generally recommended, without what using LiDAR data for saltmarsh vegetation

510   mapping may be useless (Hladik and Alber, 2012). In the present study, the way LiDAR data were processed is thus the most probable explanation for the negative effect of adding the LiDAR-derived DEM band on map accuracy.

One way to improve the overall accuracy of the classification in this study would be to merge training samples into broader vegetation classes, defining the groups at a higher

515   hierarchical level in the typology. Merged samples are known to give a better spectral representation of the vegetation class as a whole (Janssen, 2001), as shown by the high classification accuracies in Belluco *et al.*, 2006. This, however, would be at the expense of important information in regards to the vegetation groups. Accordingly, merging vegetation records into coarser groups (i.e., C-D low-mid schorre communities for the 5-group, and A-B

520   top level and high schorre communities for the 4 group mapping) overall enhanced map accuracies. In addition, combining clusters E (high slikke *Spartina maritima* swards) and F (high slikke *Spartina anglica* pioneer communities) could further decrease confusion amongst pixels and increase spectral differentiation and accuracy mapping of the slikke from the intermediate levels of the saltmarsh, at the expense of distinguishing between the groups E

525   and F. The general trend of the classification maps shows that the accuracy results become highly degraded when finer vegetation groups are distinguished coupled with reduced ground information. As finer vegetation groups may occupy a smaller area on the study site, our systematic field sampling design resulted in a smaller number of records within these vegetation groups. For instance, vegetation groups A and D were respectively represented by

530   42 and 51 records, leading to a maximum number of 22 and 31 records for map training after the removal of the 20 validation record. A 10% sub-sample of training records is thus insufficient to map these vegetation groups. As suggested above, a stratified field sampling i.e., sampling of previously defined vegetation groups, would help increase the sampling

effort in vegetation groups occupying small areas but could lead to the omission of unknown

535   vegetation types.

5.   Conclusion and Perspectives

Although the reliability of the final map can be improved by several methods, the approach developed in this study demonstrates that vegetation data-sets that are not initially designed in

540   mapping purpose (i.e. systematic rather than stratified sampling, ca. 5m-accurate record positioning) can be used in combination with rather easily acquired and processed multi-temporal multispectral imagery to create adequate saltmarsh vegetation maps. The uniqueness of this study also lies within the robust data-set of ground referenced data covering the entire site, a rich source of information permitting to create a thorough vegetation typology

545   (phytosociological associations) of the Reserve. Decreasing the number of vegetation records altered classification accuracy, proving that large ground data-sets are required for such a mapping approach to be efficient. Field data resulting from the fine scale systematic sampling scheme used in this study would hardly be acquired at larger scales. Nevertheless, providing that a sufficient amount of vegetation records and corresponding pixels per vegetation group

550   are available, our approach can be transferred to other saltmarshes even on larger areas such as the entire Arcachon Bay. Despite their lower spectral accuracy, compared to radar or hyperspectral images, multispectral images represent an interesting alternative providing that they are acquired at several dates. Our results also provide further evidence of the negative effects of including LiDAR data without any correction for the mapping of vegetated

555   saltmarsh habitats (Fernandez-Nunez *et al.*, 2017).

Quantitative, accurate, and repeatable observations of vegetation distribution over time in saltmarshes are highly important for monitoring purposes. Such observations must cover spatial and temporal scales, and remote sensing techniques are therefore ideally suited for this

task. The ability for repeated data acquisition of remotely sensed imaging coupled with the

560   accurately determined spectral signatures of vegetation groups can therefore be used to assess

spatial changes in the distribution of vegetation over time.

570

References

Adam, P., 1990. Saltmarsh Ecology. Cambridge University Press, Cambridge, UK, 461 pp.

Andresen, T., Mott, C., Zimmermann, S., Schneider, T., Melzer, A., 2002. Object-oriented information extraction for the monitoring of sensitive aquatic environments. IEEE International 5, 3083–

575   3085.

Ballanti, L., Byrd, K.B., Woo, I., Ellings, C., 2017. Remote Sensing for Wetland Mapping and Historical Change Detection at the Nisqually River Delta. Sustainability, 9: 1919.

Belluco, E., Camuffo, M., Ferrari, S., Modenese, L., Silvestri, S., Marani, A., Marani, M., 2006. Mapping salt-marsh vegetation by multispectral and hyperspectral remote sensing. Remote

580   Sensing of Environment, 105: 54-67.

Bertness, M.D., Ewanchuk, P.J., 2002. Latitudinal and Climate-driven Variation in the Strength and Nature of Biological Interactions in New England Salt Marshes. Oecologia, 132 : 392-401.

585

Bilodeau, C. 2010. Apports du LIDAR à l'étude de la végétation des marais salés de la Baie du Mont Saint Michel. Domain.stic.geop. Université Paris-Est, 2010. French. <NNT : 2012PEST1007>. <tel-00587416>.

Boorman, L.A., 1995. Sea level rise and the future of the British coast. Coastal Zone Topics: Process, Ecology and Management, 1: 10-13.

Boorman, L.A. 2003. Saltmarsh Review. An overview of coastal saltmarshes, their dynamic and sensitivity characteristics for conservation and management. JNCC Report 334. JNCC, Peterborough, 114 pp.

590

Bromberg, G.K., Silliman, B.R., Bertness, M.D., 2009. Centuries of human-driven change in salt marsh ecosystems. Annual Review of Marine Science, 1: 117-141.

Byrd, K.B., O'Connell, J.L., Di Tommaso, S., Kelly, M., 2014. Evaluation of sensor types and environmental controls on mapping biomass of coastal marsh emergent vegetation. Remote Sensing of Environment, 149: 166–180.

595

Byrd, K.B., Ballanti, L., Thomas, N., Nguyen, D., Holmquist, J.R., Simard, M., Windham-Myers, L., 2018. A remote sensing-based model of tidal marsh aboveground carbon stocks for the conterminous United States. ISPRS Journal of Photogrammetry and Remote Sensing, 139: 255–271.

600

Chapman, V.J., 1976. Coastal Vegetation, second ed. Pergamon Press, Oxford, pp. 292.

Chust, G., Galparsoro, I., Borja, Á., Franco, J., Uriarte, A., 2008. Coastal and estuarine habitat mapping, using LIDAR height and intensity and multi-spectral imagery. Estuarine, Coastal and Shelf Science, 78: 633-643.

Collin, A., Long, B., Archambault, P., 2010. Salt-marsh characterization, zonation assessment and mapping through a dual-wavelength LiDAR. Remote Sensing of Environment, 114: 520-530.

605

Congalton, R.G., 1991. A review of assessing the accuracy of classification of remotely sensed data. Remote Sensing of Environment, 37: 35-46.

de Mendiburu F., 2016. agricolae: Statistical Procedures for Agricultural Research. R package version 1.2-4. https://CRAN.R-project.org/package=agricolae

610 Dray, S. and Dufour, A.B. (2007): The ade4 package: implementing the duality diagram for ecologists. Journal of Statistical Software. 22(4): 1-20.

Dufrêne, M., Legendre, P., 1997. Species assemblages and indicator species: the need for a flexible asymmetrical approach. Ecological Monographs, 67(3): 345-366.

Fernandez-Nunez, M., Burningham, H., Ojeda Zujar, J., 2017. Improving accuracy of LiDAR-derived

615 digital terrain models for saltmarsh management. Journal of Coastal Conservation, 21: 209-222.

Hill, D., Fasham, M., Tucker, G., Shewry, M., Shaw, P., 2005. Handbook of biodiversity methods: survey, evaluation and monitoring. Cambridge University Press

Hirano, A., Madden, M., Welch, R., 2003. Hyperspectral image data for mapping wetland vegetation. Wetlands, 23: 436–448.

620 Hladik, C., 2012. Use of Remote Sensing Data for Evaluating Elevation and Plant Distribution in a Southeastern Saltmarsh. Ph.D. Thesis, The University of Georgia: Athens, Georgia.

Hladik, C., Alber, M., 2012. Accuracy assessment and correction of a LIDAR-derived salt marsh digital elevation model. Remote Sensing of Environment, 121: 224-235.

Hladik, C., Schalles, J., Alber, M., 2013. Salt marsh elevation and habitat mapping using hyperspectral

625 and LIDAR data. Remote Sensing of Environment, 139: 318-330.

Janssen, J.A.M. 2001. Monitoring of salt-marsh vegetation by sequential mapping. Ph.D. Thesis. Faculty of Science, University of Amsterdam: Netherlands.

Kelly, N.M., 2001. Changes to the landscape pattern of coastal North Carolina wetlands under the Clean Water Act, 1984–1992. Landscape Ecology, 16: 3-16.

630 Kelly, N.M., Tuxen, K., 2009. Ch. 15: Remote Sensing Support for Tidal Wetland Vegetation Research and Management. In: Yang, X. (Ed.), Remote Sensing and Geospatial Technologies for Coastal Ecosystem Assessment and Management. Springer-Verlag Berlin Heidelberg, pp. 341-363.

Klemas, V., 2011. Remote sensing of wetlands: case studies comparing practical techniques. Journal of Coastal Research, 27: 418–427.

Kulawardhana, R.W., Popescu, S.C., Feagin, R.A., 2014. Fusion of lidar and multispectral data to quantify salt marsh carbon stocks Remote Sensing of Environment, 154: 345–357.

Kulawardhana, R.W., Feagin, R.A., Popescu, S.C., Boutton, T.W., Yeager, K.M., Bianchi, T.S., 2015. The role of elevation, relative sea-level history and vegetation transition in determining carbon distribution in *Spartina alterniflora* dominated salt marshes. Estuarine, Coastal and Shelf Science, 154: 48e57.

Kulawardhana, R.W., Popescu, S.C., Feagin, R.A., 2017. Airborne lidar remote sensing applications in non-forested short stature environments: a review. Annals of Forest Research, 60: 173-196.

Lafon, V. Clos, G., Ducrot, D., Dehouck, A., Regniers, O., 2014. Multi-temporal and multi-sensor classification applied to intertidal flat mapping. IGARSS 2014, 13-18 juillet 2014, Quebec, Canada.

Lefeuvre, J.C., Laffaille, P., Feunteun, E., Bouchard, V., Radureau, A., 2003. Biodiversity in salt marshes: from the patrimonial value to the ecosystem functioning. The case study of the Mont Saint-Michel bay. Comptes Rendus Biologies, 326 (1): 125-131.

Luque, S., Pettorelli, N., Vihervaara, P., Wegmann, M., 2018. Improving biodiversity monitoring using satellite remote sensing to provide solutions towards the 2020 conservation targets. Methods in Ecology and Evolution, 9 : 1784-1786.

Marani, M., Belluco, E., D'Alpaos, A., Defina, A., Lanzoni, S., Rinaldo, A., 2003. On the drainage density of tidal networks. Water Resources Research, 39: 1040.

McFeeters, S.K., 1996, The use of normalized difference water index (NDWI) in the delineation of open water features. International Journal of Remote Sensing, 17: 1425–1432.

McRoberts, R. E., Wendt, D. G., Nelson, M. D., Hansen, M. H., 2002. Using a land cover classification based on satellite imagery to improve the precision of forest inventory area estimates. Remote Sensing of Environment, 81 (1): 36–44.

Oksanen, J., Blanchet, F.G., Kindt, R., Legendre, P., Minchin, P.R., O'Hara, R.B., Simpson, G.L., Solymos, P., Stevens, M.H.H, Wagner, H.H., 2016. vegan: Community Ecology Package. R package version 2.3-5. https://CRAN.R-project.org/package=vegan

Owers, C., Rogers, K., Woodroffe, C.D., 2016. Identifying spatial variability and complexity in wetland vegetation using an object-based approach. International Journal of Remote Sensing, 37: 4296-4316.

665   Ozesmi, S.L., Bauer., M.E., 2002. Satellite remote sensing of wetlands. Wetland Ecology Management, 10: 381-402.

Pennings, S.C., Callaway, R.M., 1992. Salt marsh plant zonation: the relative importance of competition and physical factors. Ecology, 73: 681e690.

R Core Team, 2016. R: A language and environment for statistical computing. R Foundation for
670   Statistical Computing, Vienna, Austria. URL https://www.R-project.org/.

Rapinel, S., Hubert-Moy, L., Clément, B., 2015. Combined use of LiDAR data and multispectral earth observationimagery for wetland habitat mapping. International Journal of Applied Earth Observation and Geoinformation, 37: 56–64.

Rapinel, S., Rossignol, N., Hubert-Moy, L., Bouzillé, J.-B., Bonis, A., 2018. Mapping
675   grassland plant communities using a fuzzy approach to address floristic and spectral uncertainty. Applied Vegetation Science, DOI: 10.1111/avsc.12396.

Reveillas, M., Alfonsi, E., Alard, D., 2012. Typologie et cartographie des habitats naturels du compartiment sous influence tidale –RNN des Prés salés d'Arès et de Lège Cap-Ferret. University of Bordeaux. ONCFS, 61p.

680   Roberts, D.W., 2016. labdsv: Ordination and Multivariate Analysis for Ecology. R package version 1.8-0. https://CRAN.R-project.org/package=labdsv

Robins, P.E., Skov, M.W., Lewis, M.J., Giménez, L., Davies, A.G., Malham, S.K., Neill, S.P., McDonald, J.E., Whitton, T.A., Jackson, S.E., Jago, C.F., 2016. Impact of climate change on UK estuaries: A review of past trends and potential projections. Estuarine, Coastal and Shelf
685   Science, 169: 119-135.

Rosso, P. H., Ustin, S. L., Hastings, A., 2005. Mapping marshland vegetation of San Francisco Bay, California, using hyperspectral data. International Journal of Remote Sensing, 26: 5169-5191.

Rosso, P. H., Ustin, S. L., Hastings, A., 2006. Use of lidar to study changes associated with Spartina invasion in San Francisco Bay marshes. Remote Sensing of Environment, 100: 295-306.

690   Rouse, J.W, Haas, R.H., Scheel, J.A., Deering, D.W., 1974. Monitoring Vegetation Systems in the Great Plains with ERTS. Proceedings, 3rd Earth Resource Technology Satellite (ERTS) Symposium, vol. 1, pp. 48-62.

Schmidt, K.S., Skidmore, A.K., Kloosterman, E.H., van Oosten, H.H., Kumar, L., Janssen, J.A.M., 2004. Mapping coastal vegetation using an expert system and hyperspectral imagery.
695   Photogrammetric Engineering and Remote Sensing, 70(6): 703-715.

Silvestri, S., Marani, M., 2004. Salt-Marsh Vegetation and Morphology: Basic Physiology, Modelling and Remote Sensing Observations. In: The Ecogeomorphology of Tidal Marshes Coastal and Estuarine Studies, Ch. 2, pp. 5-24.

Smith, G., Spencer, T., Murray, A.L., French., J.R., 1998. Assessing seasonal vegetation change in
700   coastal wetlands with airborne remote sensing: an outline methodology. Mangroves and Salt Marshes, 2: 15–28.

Stankiewicz K, Dabrowska-Zielinska, K., Gruszczynska, M., Hosciło A., 2003. Mapping vegetation of a wetland ecosystem by fuzzy classification of optical and microwave satellite images supported by various ancillary data. In: Owe M., D'Urso G., Toulios L. (Eds) SPIE. Remote Sensing for
705   Agriculture, Ecosystems, and Hydrology IV, pp 351-361.

Tuxen, K., Schile, L.M., Kelly, M., Siegel, S.W., 2008. Vegetation Colonization in a Restoring Tidal Marsh: A Remote Sensing Approach. Restoration Ecology, 16(2): 313–323.

Tuxen, K., Schile, L., Stralberg, D., Siegel, S., Parker, T., Vasey, M., Callaway, J., Kelly, M., 2011. Mapping changes in tidal wetland vegetation composition and pattern across a salinity gradient
710   using high spatial resolution imagery. Wetlands Ecology Management, 19:141-157.

Van Beijma, S., Comber, A., Lamb, A., 2014. Random forest classification of salt marsh vegetation habitats using quad-polarimetric airborne SAR, elevation and optical RS data. Remote Sensing of Environment, 149: 118-129.

Viera, A.J., Garrett, J.M., 2005. Understanding Interobserver Agreement: The Kappa Statistic. Family
715   Medicine, 37(5): 360-3.

Wang C., Menenti, M., Stoll, M.P., Belluco, E., Marani, M., 2007. Mapping mixed vegetation communities in salt marshes using airborne spectral data. Remote Sensing of Environment, 107: 559-570.

Zhang, M., Ustin, S.L., Rejmankova, E., Sanderson, E.W., 1997. Monitoring Pacific Coast Saltmarshes Using Remote Sensing. Ecological Applications, 7(3): 1039-1053.

Zhang, Y., Lu, D., Yang, B., Sun, C., Sun, M., 2011. Coastal wetland vegetation classification with a Landsat Thematic Mapper image. International Journal of Remote Sensing, 32(2): 545-561.

720

Figures

Fig. 1. Map of the Arcachon Bay (left) showing the location of the study area in Southwestern France. The study site is shown outlined in white (right). Image source: IGN BD ORTHO ® 50cm.

Fig. 2. (A) Hierarchical Classification performed on the [452 records x 35 species] data table. The red line indicates the level where the dendrogram was cut to define six clusters (named A-F) used for the associations. Indicator species' codes are provided above the branches of each cluster group. Species richness is shown for each group. (B) Correspondence analysis on the F1-F2 factorial plan of the records showing the vegetation groups (defined in the Hierarchical Classification). Habitat turnover from high to low marsh is visualized by the arrow. See Table S1 in Electronic Supplementary Material for complete species' names and corresponding codes.

Fig. 3. Maximum likelihood classification maps (after application of the post majority filter), obtained using 100% of the remaining available records for the training groups (A) only with optical layers (overall accuracy: 75.5%) and (B) with optical and digital elevation model layers (overall accuracy: 73.6%). The six vegetation groups in addition to water bodies (channels and hunting ponds), sand, and mudflats are featured. No LiDAR data were available for water bodies and mudflats, which do not appear on the resulting map (B)

Fig. 4. Comparison of obtained K values for the six, five, and four vegetation groups with (dashed lines) and without (solid lines) digital elevation model layer. Bars represent the standard error of the K values for the classifications.

Fig. 5. Maximum likelihood classification maps demonstrating results for 100% (top), 50% (middle), and 20% (bottom) of the remaining available records for the training groups for the six (A, D, G), five (B, E, H), and four (C, F, I) thematic classes. Only classifications including optical layers are shown.

Tables

Table 1. Phytosociological categories (alliance or association) and Natura 2000 habitat codes (N2000 Code) for the identified vegetation groups. Group codes and generic names are provided for each determined thematic class in addition to the total number of ground records and the maximal number of records remaining for map training.

Table 2. Interactive Supervised Classification (ISC) error matrix of the final map using 100% of the remaining available records for the training groups (A) only with optical layers and (B) with optical and digital elevation model (DEM) layers. Columns represent the reference data (what the pixel actually was based on validation data) and rows represent the image data (what the pixel was classified as). Shaded cells show the correctly classified pixel observations for each association. Results are in total number of pixels, while the producer and user's accuracy are in percentage.

Table 3. Overall accuracy assessment (%) of the classification results for six, five, and four vegetation groups, with and without digital elevation model (DEM) layer.